Scientific Papers. Series E. Land Reclamation, Earth Observation & Surveying, Environmental Engineering. Vol. IX, 2020
Print ISSN 2285-6064, CD-ROM ISSN 2285-6072, Online ISSN 2393-5138, ISSN-L 2285-6064

IN SITU GEOMETRIC CALIBRATION OF A HYBRID SYSTEM COMPOSED BY UAV/GNSS/IMU/AERIAL CAMERA AND LiDAR

Gabriel POPESCU[1], Octavian Laurentiu BALOTA[1], Daniela IORDAN[1], Daniel ILIE[2]

[1]University of Agronomic Sciences and Veterinary Medicine of Bucharest, 59 Marasti Blvd., District 1, Bucharest, Romania
[2]Prosig Expert SRL, 208B Basarabia Blvd., District 2, Bucharest, Romania

Corresponding author email: gabrielpopescu2013@gmail.com

Abstract

The paper aimed to present the in situ geometric calibration of a hybrid system composed by an Unmanned Aerial Vehicle (UAV) which is equipped with Global Navigation Satellite System (GNSS), Inertial Measurement Unit (IMU), aerial optical camera and a LiDAR. For a realistic representation of a geographic area by combining optical and LiDAR data, captured with UAV, we need first of all to calibrate the both sensors (passive and active) optical and LiDAR. In our study, we used a digital camera, and influences of focal length and principal point coordinates were needed to be treated as unknown parameters for adjustment purposes. We used LiDAR data for in situ calibration of digital camera and the test site which was selected in the project area and control points have been obtained from LiDAR point cloud and intensity data. The in-situ calibration of digital camera was based on a large number of tie points and the LiDAR derived control points using a conventional bundle block adjustment with self-calibration. The in situ geometric calibration of our hybrid system, was achieved and verified for validation in a test area, near Bucharest, checking the spatial data sets used (optical and LiDAR) and for final data validation we used the ground truth, given by GNSS measurements in the field.

Key words*: calibration, GNSS, LiDAR, photogrammetry, UAV.*

INTRODUCTION

The concept of *in situ* system calibration (also called self-calibration which originates from close range applications) for aerial optical cameras has been clearly demonstrated in the last decades, and nowadays most final system calibrations provided by aerial camera manufacturers, particularly for digital cameras, are produced by aerial, *in situ* approaches. Many examples of geospatial accuracies provided by *in situ* calibrations may be found in few scientific articles of analytical and digital photogrammetry (Brown, 1969; Merchant et al., 2012).

The camera calibration process involves the geometric calibration, resolution determination and radiometric calibration of camera. In this paper we are referring to geometric calibration only.

The laboratory calibration is a standard method for analog airborne frame cameras. The interior camera geometry, focal length, principle point location and lens distortion parameters are included in the calibration certificate of the digital camera. As a general concept, all those parameters which were not corrected for in the image provided to the user should be treated as unknown parameters in the calibration computations. The calibration report must state the mathematical model used to represent the interior orientation of the camera, the estimates of parameter values of the model and estimates of errors in the adjusted parameters.

Camera calibration reports provided by digital aerial camera manufacturers also provide a rich source of high-quality results.

In situ system calibration requires a calibration field with signalized control points of high accuracy and so the camera calibration parameters can be estimated in standard airborne flight configuration with the camera positions given by GNSS.

Another approach for the *in situ* camera calibration is used to estimate the interior orientation parameters of the digital camera used in the flight conditions which does not require a calibration test field and also neither traditional ground control points (Mitishita et al., 2017). So, the LiDAR dataset was used as a control of position information for the photogrammetric survey performed by the

direct sensor orientation technology. Using the collinearity equations and Least Squares Bundle Block Adjustment, the theoretical collinearity condition among the point image, camera exposition station and point object was in practice recovered by additional parameters related to lens distortions, coordinates of principal point and the sensor distortion. So, in this case, the *in situ* camera calibration must use LiDAR Derived Control Points (LCPs) and a small sub-block of images extracted from the entire image block obtained in the aerial survey.

Light Detection and Ranging (LiDAR) is a remote sensing technology that has been widely used in many fields, for example: canopy cover estimations, Doppler measurements (Scotti et al., 2015), oceanological monitoring of fishing areas (Chernook et al., 2014), city planning and disaster management (Chen et al., 2014), etc. The data collected by LiDAR system could be processed into the LiDAR Digital Surface Model (DSM) which contains not only Digital Elevation Model (DEM) information but also all the objects lying on the Earth's surface. The elevation information helps to classify different objects of with different heights, such as trees, buildings and so on. LiDAR has been shown to be a very useful tool for classification purposes. LiDAR data and aerial images, both captured with the same UAV, have their own unique advantages and disadvantages and it is natural to integrate those two data sets for a good realistic representation of a geographic area in terms of horizontal and vertical accuracy. Compared with aerial images, LiDAR data provide more accurate height information but less accurate boundaries. Aerial images provide more extensive planimetric information such as high-resolution texture and colour information. Although 3D height information can be estimated from one or several images by the use of several photogrammetric methods, the height information extracted from aerial images is still relatively less accurate, and the experimental results indicate that this combination improves the overall accuracy.

MATERIALS AND METHODS

In this paper, it is presented a hybrid system based on UAV equipment using a combination of two technologies LiDAR and photogrammetry. UAV was a hexacopter DJI MATRICE M600 PRO with vertical take-off and landing which are collecting high density of LiDAR points and RGB digital colour aerial images.

The UAV system, presented in this paper, was realized within the project “System for rapid monitoring and interactive mapping”, co-financed from the European Regional Development Fund through the Operational Program Competitiveness 2014-2020, financing contract 124/2016 concluded with the National Research and Innovation Authority as Intermediate Body (OI), on behalf of the Romanian Ministry of European Funds (MFE) as Managing Authority (MA) for the Competitiveness Operational Program.

The specific objectives and results of the project were the development of advanced and accurate methodologies based on UAV systems equipped with LiDAR and photographic camera for obtaining several geospatial products like "digital topographic map in a GIS structure", "realistic representation of a geographical area" and "landscape change detection complete report".

For these products were studied the technical conditions and the optimum steps in the technological process of their generation. One of these steps was geometric calibration, and the results of this research are presented in the next chapter. The DJI MATRICE M600 PRO drone, used in our study (Figure 1), is a professional hexacopter drone, being one of the most efficient in terms of flight performance (high stability and transport capacity). The pre-installed arms reduce the time required to prepare the UAV system for flight.

Figure 1. Hexacopter DJI MATRICE M600 PRO

The ability of these arms to fold, helps in easy transport but also in speeding up the drone mounting. In addition, the ability of rotor propellers to tighten emphasizes these advantages over other air platform solutions available on the market.

The DJI MATRICE M600 PRO platform was equipped with the latest technologies of DJI, being from this point of view a latest generation product. The platform is equipped with the A3 Pro Flight Controller, radio remote control and iPAD PRO 9.7 inches tablet, Lightbridge 2 HD transmission system, smart battery charging station and high-performance flight batteries. The system also includes flight control software: one for the iPAD PRO tablet, called DJI GO and one for the computer, for connecting systems of the Drone (Lightbridge, D-RTK, ProLink Model etc.), called DJI Assistant 2.

The integrated LiDAR on the same drone, was designed for the acquisition of LiDAR data with high accuracy (between ± 2 cm and ± 5 cm RMSE at an average acquisition distance of 40 m and 100 m, respectively), and supplemented with RGB information for each point. Our LiDAR system was composed of several subassemblies, as follows:

- System platform, CPU integrator developed by the Phoenix LiDAR Systems (Figure 2) for the LiDAR-GNSS-IMU assembly, which has the function of correlating in real time the data acquired from all the sensors of the system.

Figure 2. LiDAR-IMU-CPU-Camera

- GNSS navigation system (Figure 3) is a dual frequency RTK-GNSS system, with GPS / GLONASS support. The DJI D-RTK system used for the UAV system is partially used, because the LiDAR system has its own GNSS subassembly composed by two GNSS antennas. This GNSS is also used for improving the heading and the alignment of the entire system. This kind of GNSS subsystem is used in correlation with a medium or low accuracy IMU sensor (for example like ADIS sensors). When the system has a precise IMU sensor, it can be used just a single GPS antenna.

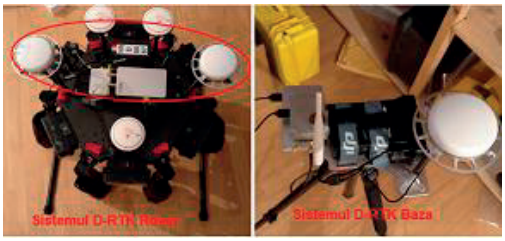

Figure 3. The DJI D-RTK system (Rover and Base)

- IMU System - Analog Devices model ADIS 16488 (IMU-14) or STIM (IMU-27), integrated into the system platform (CPU).
- Velodyne VLP-16 PUCK or Velodyne VLP32C LiDAR sensors for acquiring the point cloud.
- Photo Camera Sony A6000 and Sony A7R II (shown in Figure 4) are used to capture RGB images for each point determined by LiDAR technology.

Figure 4. Photo Cameras Sony A6000 (left) and Sony A7R II (right)

The images thus acquired can be used for photogrammetric products (photograms, stereo-restitution, orthophotos), if the flight of data retrieval is designed in such way to ensure the necessary longitudinal and transversal coverage of the images.

RESULTS AND DISCUSSIONS

For testing different parameters for fly, three flights were designed from different heights with the DJI M600 VLP 16 LiDAR system.

The first day that flew was when the average temperature was 11ºC, the wind speed was

6 km/h, the visibility was 7.6 km, the humidity was around 70 mmHg. On this first day the flight was made at a flight height of the drone set at 60 m, so chosen to have visibility between operators and the drone, but also between the drone and the WIFI long range antenna.

Another flight was made at a flight height of 40 m, on a length of 1.6 km, with LIDAR and optical data being acquired for objects such as roads, houses, cars, electric poles, high and low vegetation.

We concluded that the interior orientation and the mounting parameters can vary over time. For instance, the interior orientation parameters can change under flight conditions due to the effects of temperature and pressure, and to improve the accuracy of the direct sensor orientation, the system calibration (including the interior orientation and mounting parameters) is recommended before or after each photogrammetric mission.

Internal parameters, of a digital camera calibration, are: the focal length in pixels, the principal point coordinates, skew coefficient defining the angle between the x and y pixel axes (stored in the scalar) and the image distortion coefficients (radial and tangential distortions).

A scene view, which is formed by projecting 3D points into the image plane using a perspective transformation, is shown in Figure 5 (https://docs.opencv.org/2.4/index.html).

If we consider a point „P" in the space-object and its correspondent point „p" on the image, we have the following formula in matriceal form (OpenCV, 2019):

$$\mathbf{s * p = A * [\,R|T\,] * P} \qquad (1)$$

$$s\begin{bmatrix} u \\ v \\ 1 \end{bmatrix} = \begin{bmatrix} f_x & 0 & c_x \\ 0 & f_y & c_y \\ 0 & 0 & 1 \end{bmatrix} \begin{bmatrix} r_{11} & r_{12} & r_{13} & t_1 \\ r_{21} & r_{22} & r_{23} & t_2 \\ r_{31} & r_{32} & r_{33} & t_3 \end{bmatrix} \begin{bmatrix} X \\ Y \\ Z \\ 1 \end{bmatrix}$$

where:

(X, Y, Z) are the coordinates of a 3D point in the world coordinate space;

(u, v) are the coordinates of the projection point in pixels;

A is a camera matrix, or a matrix of intrinsic parameters;

(c_x, c_y) is a principal point that is usually at the image centre;

(f_x, f_y) are the focal lengths expressed in pixel units.

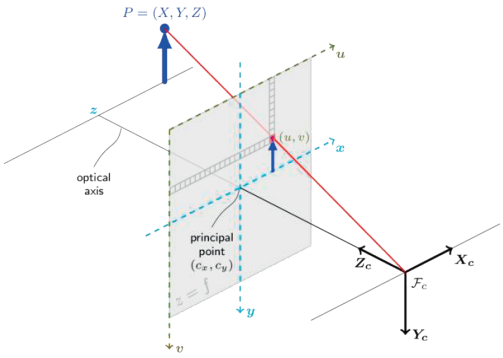

Figure 5. Coordinate systems used in perspective transformation for digital camera calibration (OpenCV, 2019):

When an image from the camera is scaled by a factor "s", all of these parameters should be scaled (multiplied/divided, respectively) by the same factor. The matrix of intrinsic parameters does not depend on the scene viewed. The joint rotation and translation matrix **[R|T]** are called a matrix of extrinsic parameters. It is used to describe the camera motion around a static scene, or vice versa, rigid motion of an object in front of a still camera. That is, translates coordinates of a point to a coordinate system, fixed with respect to the camera. The transformation above is equivalent to the following, when $z \neq 0$:

$$\begin{bmatrix} x \\ y \\ z \end{bmatrix} = R \begin{bmatrix} X \\ Y \\ Z \end{bmatrix} + \mathbf{T} \qquad (2)$$

$$x' = x/z$$
$$y' = y/z$$
$$u = f_x * x' + c_x$$
$$v = f_y * y' + c_y$$

Because the lenses of the camera objective, usually have some distortion, mostly radial distortion and slight tangential distortion, the above formula is extended, as follows (OpenCV, 2019):

$$\begin{bmatrix} x \\ y \\ z \end{bmatrix} = R \begin{bmatrix} X \\ Y \\ Z \end{bmatrix} + T \quad (3)$$

$$x' = x/z$$
$$y' = y/z$$
$$x'' = x' \frac{1+k_1r^2+k_2r^4+k_3r^6}{1+k_4r^2+k_5r^4+k_6r^6} + 2p_1x'y' + p_2(r^2+2x'^2)$$
$$y'' = y' \frac{1+k_1r^2+k_2r^4+k_3r^6}{1+k_4r^2+k_5r^4+k_6r^6} + p_1(r^2+2y'^2) + 2p_2x'y'$$
where $r^2 = x'^2 + y'^2$
$$u = f_x * x'' + c_x$$
$$v = f_y * y'' + c_y$$

Finally, we have the output vector of distortion coefficients (**k_1, k_2, p_1, p_2[, k_3[, k_4, k_5, k_6]]**) of 4, 5, or 8 elements.

These coefficients of camera calibration **k_1, k_2, k_3, k_4, k_5** and **k_6** are radial distortion coefficients; **p_1** and **p_2** are tangential distortion coefficients and higher-order coefficients are not considered in this application.

For example, in Figure 6, are shown two common types of radial distortion: barrel distortion (typically **$k_1>0$**) and pincushion distortion (typically **$k_1<0$**).

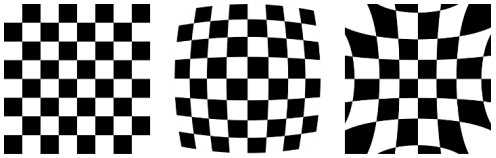

No distorsion Positive distorsion Negative distorsion

Figure 6. Two common types of radial distortion

The calibration of a digital camera is usually performed in laboratory and the determined parameters may not reflect the flight conditions due to the effect of temperature and air pressure. For this reason, these parameters are frequently determined or refined with *in situ* calibration using a test field with distributed control points of high accuracy.

In present, UAVs use the combination of imaging and navigation sensors, such as digital camera, LiDAR, GNSS and IMU. Usually, these systems use direct geo-referencing for imaging sensor orientation, and the calibration of individual sensors and the relation between them is very important because any difference between assumed calibration parameters and physical parameters can cause significant errors in object space. The geometric sensor calibration parameters for camera, estimated by adjustment, are: 2D coordinates of principal point, principal distance and image distortion parameters (number of radial and tangential distortion coefficients). In Figure 7, we presented an extract from the calibration certificate of the Sony A6000 optical camera, a component of the LIDAR SCOUT system, which is part of the UAV assembly, issued by Phoenix LiDAR Systems from USA, the distributor company of the camera.

Camera 0 Type:	Sony a6000	
Camera 0 Serial #:	6450763	
	X (width)	**Y (height)**
Sensor Size (mm)	23.500	15.6670
Pixel Size (px)	6000	4000
Principal Point (px)	2976.670	1981.860
Focal Length (px)	4127.793	4127.793

	k1	**k2**	**k3**
Radial	-0.008	-0.001	0.007

	p1	**p2**
Tangential	0	0

Figure 7. Extract from the calibration certificate of the Sony A6000 optical camera

In Figure 8, we presented an RGB image before (a) and after (b) geometric calibration using *Spatial Fuser software of* Phoenix LiDAR Systems.

a) RGB image before calibration

b) RGB image after calibration

Figure 8. RGB image before (a) and after (b) calibration

If it is necessary to apply geometric corrections in a processing medium other than *Phoenix*

LiDAR Systems Spatial Fuser, it is necessary to obtain the parameters of external orientation, to restore the image retrieval mode (Figure 9).

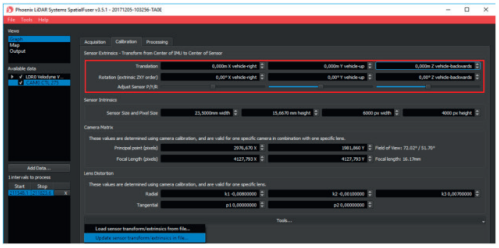

Figure 9. Obtaining the external orientation parameters for the geometric correction of the images

In our project we used also LiDAR data for *in-situ* calibration of digital camera. The test site was selected in the project area and control points were obtained from LiDAR point cloud and intensity data.

The *in situ* calibration of digital camera was based on a large number of tie points and the LiDAR derived control points using a conventional bundle block adjustment with self-calibration. The displacement vector and attitude relationship between digital camera and IMU body frame was determined by comparing the GNSS/IMU derived image orientations and the results of bundle block adjustment.

The aim of the hybrid adjustment is to simultaneously optimize the relative orientation and absolute orientation (georeference) of the LiDAR and image data. The sensor orientations can be optimized by minimizing the discrepancies within the overlap area of flight strips and images and with respect to ground truth data, if it is available. The measurement process is rigorously modelled using the original measurements of the sensors (scanner: polar measurements, camera: image coordinates) and the flight trajectory of the drone. This way, systematic measurement errors can be corrected where they originally occur. Both, LiDAR scanner and photo camera, can be fully re-calibrated by estimating their interior calibration and mounting parameters (lever arm, boresight angles). Systematic measurement errors of the flight trajectory can be corrected individually for each flight strip.

The geometric sensor calibration parameters for LiDAR, estimated by adjustment, are: range offset (bias), range scale, angle offsets (biases) and angle scales. The parameters representing the geometric corrections of the optical data are different for each image separately. These corrections are necessary to restore the image retrieval mode, along with the restoration of the LIDAR data retrieval matrix for their fusion. In this way you finally get the LIDAR point cloud with RGB information. In Figure 10, it is shown an example of the uncalibrated and incorrect data set in the Pantelimon area, made with *Portree-Prosig* software.

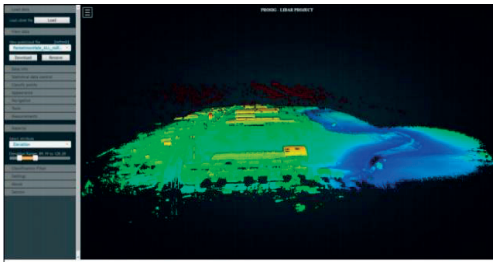

Figure 10. Presentation of the uncalibrated and incorrect data set in the Pantelimon area

The application of the point cloud calibration method is performed using the *LiDAR Tools* application. On the map used, the waveguide curvature in the flight zone is calculated by interpolating between two successive level curves. For example, in the case of flights from the Pantelimon area, the ondulation of the quasigeoid is 35.2647 meters (35.2500 m + 0.0147 m). So, we know the values of differences between the ellipsoidal quota and the normal quota in our test area. After the application of the undulating elevation values quasigeoid, results can be seen in Figure 11. The cloud of LiDAR points is considered now calibrated in the Romanian altimetric "0 Black Sea 1975", 1990 edition.

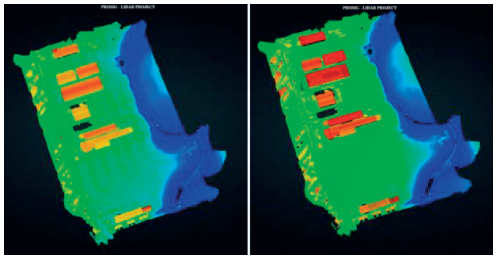

Figure 11. Transforming the LiDAR point cloud before (left side) and after (right side) applying the cvasigeoid ondulation

For calibration and correction of LiDAR data we used, also, an offline software *LiDAR Tools* installed on desktop computer that allowed us: the loading of the LiDAR point cloud in LAS format, its visualization based on the same principles as in the *Potree Prosig* on-line application, different statistical calculations and the classification of the point cloud using some quick and efficient methods (Figure 12).

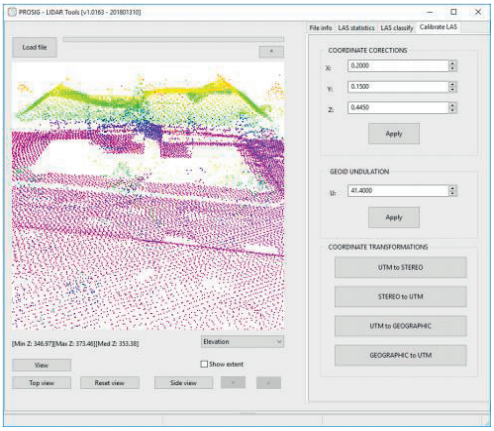

Figure 12. Interface for calibration and correction of LiDAR data

The identification of the values of the low and high Z parameters for the LAS files, is made using the *Potree-Prosig* software (Figure 13).

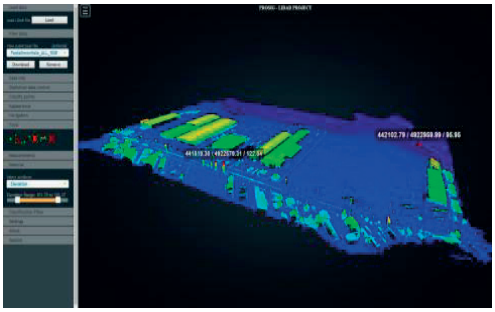

Figure 13. Identification of the values of the low and high Z parameters for the LAS file, using the *Potree-Prosig* software

Regarding the correction of LiDAR and optical data, this is done on LiDAR data, where the algorithms implemented in the *LiDAR Tools* application are applied to filter the data cloud from those points that are improbable, and the correction of optical data is done by applying on the images of the external orientation elements (rotation angles and coordinates of the images acquisition centres). Finally, the calibration performance was evaluated by analysing correlation between the estimated system parameters, the *a-posteriori* variance factor of the Least Squares Adjustment procedure and the quality of fit of the adjusted point cloud to planar/linear features before and after the calibration process.

CONCLUSIONS

The *in situ* system calibration parameters can be classified into two groups: the calibration parameters of individual sensors and the relationships between sensors. The calibration between sensors is comprised of the GNSS antenna offset (lever arm), and the determination of an offset vector and attitude difference between the IMU body frame and the imaging sensor. Combining geo-data acquired from a common platform by both sensors requires that they are in the same coordinate system. So, an approach to achieve this geo-referencing is to process each data stream independently, using the same GNSS/IMU data or by using GCPs acquired in the same datum. The D-RTK Rover system from Figure 3 (left side) contains two GNSS antennas, capable of receiving signals from satellites, both from the NAVSTAR and GLONASS constellations. In the Asia-Pacific area they are programmed to use the signals from the BEIDOU satellites as well. The D-RTK Rover system also contains a satellite data analysis processor, as well as a radio module for receiving basic corrections (DataLINK PRO 900). The D-RTK Base system is basically similar to the one installed on the drone, except that only one GNSS antenna is required for the base and not two (Figure 3, right side).
In addition, the radio module is designed to provide corrections, not receive. The power supply in the case of the basic D-RTK module is achieved by connecting it to a DJI TB47S type battery, or a similar battery.
The D-RTK system is used for precise flights, inhibiting the functionality of the A3 Pro flight GPS antennas (only for the 3 smaller GPS antennas to determine the navigation position and the course angle, with a lower accuracy).

Thus, the DJI MATRICE M600 PRO drone in this configuration can be used for geodetic applications and for scientific research applications where accuracy is a request. The D-RTK GNSS antennas can also be used for improving the accuracy of the IMU sensor (for example on LiDAR Scout 16 system). The main subassembly of those subsystems is composed by the LiDAR sensor, CPU, IMU and the optical camera which are integrated as is seen in the Figure 2. This subassembly is integrated in a single component. This is an absolute condition to obtain a good accuracy of the measured data. All the components are related to the IMU sensor through the measured offsets and the rotation angles between each coordinate system of each component.

Measurement of imagery and processing of the GNSS data and range coordinates have been conducted with a software capable of carrying the parameters of interior and exterior orientation as parameters with the possibility of application of appropriate weight constraints. Error estimates after adjustment should be provided along with the estimated standard error of unit weight. The mathematical model to be used to represent the camera's interior orientation will depend on the level of correction that will be applied to the imagery to be provided to the user. For performance evaluation of the camera calibration parameters and boresight misalignment was analysed by comparing the results of measuring points in stereo models formed using the bundle block adjustment and, respectively, the direct sensor orientation. For performance evaluation of the in situ determined camera and boresight calibration parameters were tested using independent LiDAR target points which were originally used for testing of the LiDAR data accuracy. The UAV LiDAR system calibration attained an accuracy of about 2 cm, which is better than the expected accuracy of around 5-10 cm, keeping in mind the accuracies of the hardware involved. This indicates that the proposed calibration method was efficient and accurate. For the future researching work, we shall focus on combining the mounting parameters (extrinsic parameters) and sensor parameters (intrinsic parameters) to obtain a comprehensive calibration leading to even more accurate point clouds. So, we hope to demonstrate, in the future work, that, a simultaneous calibration of mounting parameters (extrinsic) and intrinsic sensor parameters has better accuracy of the obtained LiDAR 3D point cloud combined with information from other sensors, such as RGB cameras or hyperspectral sensors, to extract more valuable information related to different applications. Exploiting the advantages of both, light detection and ranging and dense image matching, point clouds will improve the quality of the final geospatial products.

The system calibration, in principle, can be performed before or after every mission to check the quality of the mounting and interior orientation parameters. The main challenge in integrating LiDAR and dense image matching data consistently lies in proper consideration of their high variations in resolution and precision. In aerial applications, the dense image matching point cloud is typically of higher density and lower depth precision than the LiDAR data when captured at high altitude. This is due to the resolution limitation of the LiDAR beam divergence and repetition time on the one hand, and the availability of high-resolution large-frame cameras on the other.

The future tendency, is that all new generations of airborne LiDAR systems integrate a LiDAR unit and a passive imaging unit (in a single camera or multi camera fashion) in the same platform for concurrent acquisition of ranging and imagery data.

REFERENCES

Brown, D. (1969). Advanced Methods for the Calibration of Metric Camera, Final Report, Part 1, DBA Systems, Inc., Melbourne, Fla., 117 p., 1969.

Chen, Y., Cheng, L., Li, M., Wang, J., Tong, L. and Yang, K. (2014). Multiscale grid method for detection and reconstruction of building roofs from airborne LiDAR data, IEEE J. Sel. Topics Appl. Earth Observ. Remote Sens, vol.7, no. 10, pp. 4081–4094, Oct. 2014.

Chernook, V. I., Vasilyev, A. N., Goldin, Y. A., Gureev, B. A., Goryainov, V. S. and Buznikov, A. A. (2014). "Oceanological monitoring of fishing areas using Lidars" in Proc. Int. Conf. Laser Opt., Jun. 2014.

Merchant, D. C., (2012). Aerial Camera Metric Calibration - History and Status, Proceedings of ASPRS 2012 Annual Conference, Sacramento, Calif., March 19-23, 2012.

Mitishita, E., Costa, F., Martins, M. (2017). "Study of the integration of Lidar and photogrammetric datasets by in situ camera calibration and integrated sensor

orientation", The International Archives of the Photogrammetry, Remote Sensing and Spatial Information Sciences, Volume XLII-1/W1, 2017.

OpenCV dev team. Last updated on Dec 31, 2019. Sphinx 1.3.6. https://docs.opencv.org/2.4/index.html

Scotti, F., Onori, D., Scaffardi, M., Lazzeri, E., Bogoni, A. and Laghezza, F. (2015). Multi-frequency lidar/radar integrated system for robust and flexible Doppler measurements, IEEE vol. 27, no. 21, pp. 2268–2271, Jul. 28, 2015.